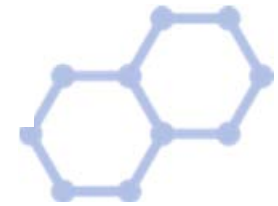


Graphene Canada2015



Theory and computation of the electronic band structures and optical absorption spectra for incommensurate tBLG and tFLG Graphene systems

Antoine Khater, Doried Ghader, Dominik Szczesniak

Institut des Molécules et Matériaux du Mans IMMM UMR 6283

Université du Maine, 72085 Le Mans, France

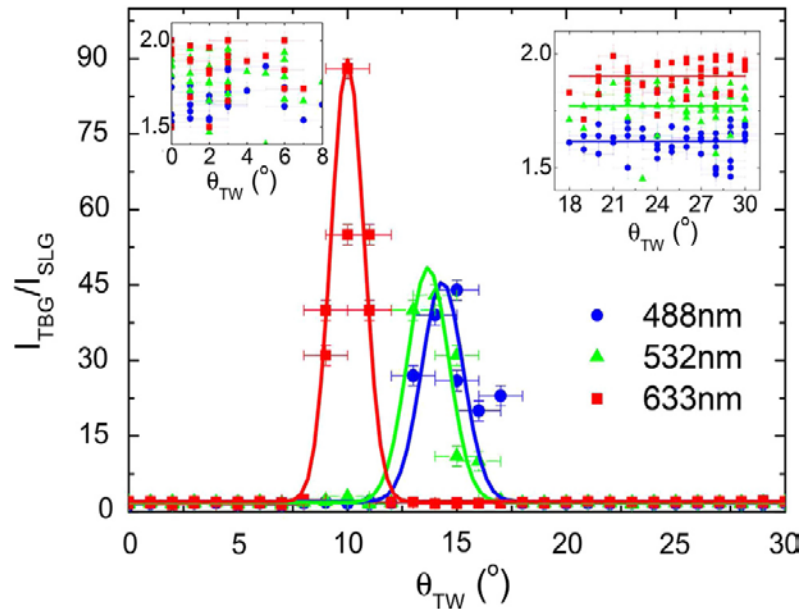


Problem: the origins of the van Hove singularities (VHS) in tBLG are not completely understood.

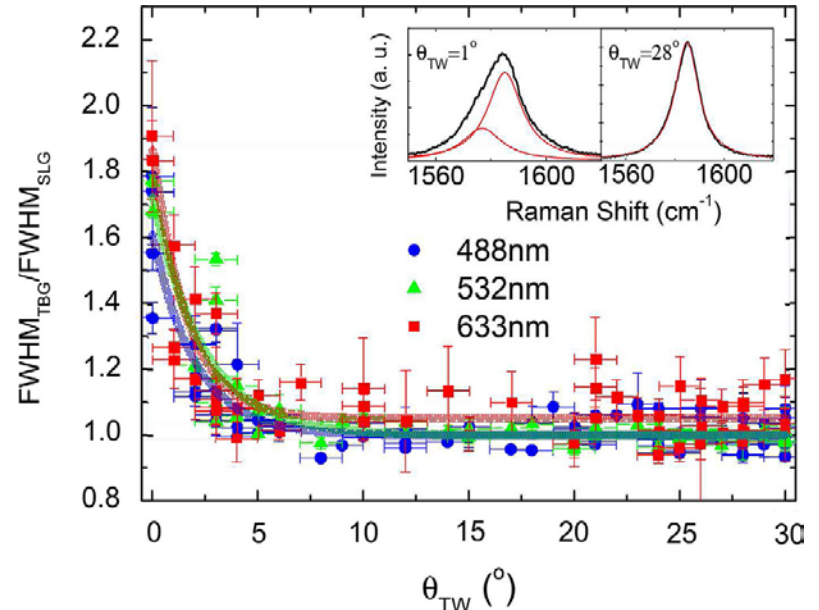
- **The van Hove singularity (VHS) in tBLG engenders a gap in the tBLG electronic band structure**
- **Interestingly the gap may be modulated as a function of the mismatch twist angle θ**

Experimental evidence for the VHS singularities and corresponding gaps

A great deal of experimental evidence for the VHS singularities and corresponding gaps exists, for example: Raman spectroscopy; the phonon frequencies give a Raman signature of the **specific tBLG**, while their linewidths provide a straightforward test for tBLG **structural homogeneity**.



Normalised resonant Raman spectra for tBLG systems, for different laser frequencies, as a function of the twist mismatch angle θ .



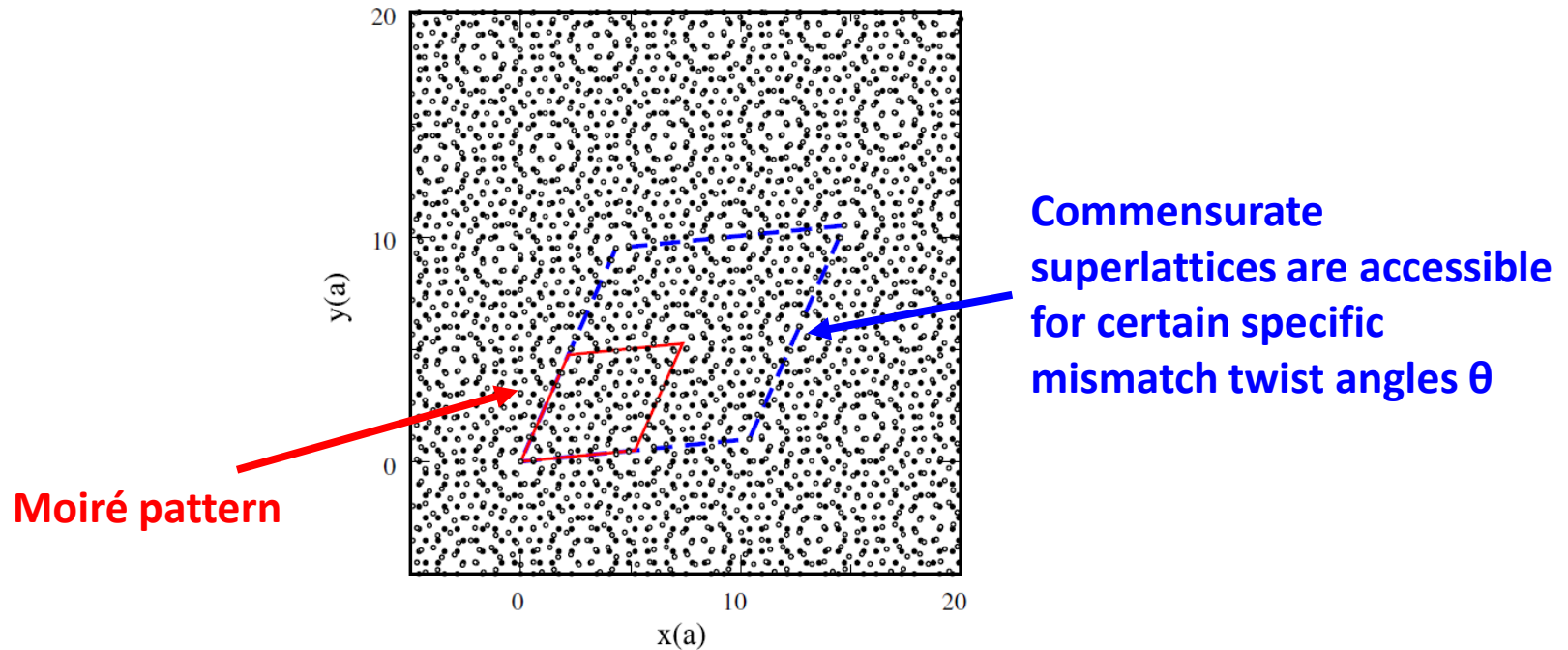
Normalised FWHM (full width at half maximum) of Raman spectra for tBLG systems, for different laser frequencies, as a function of the twist mismatch angle θ .

Intensive theoretical & computational research work in recent years

Mostly developed long-range effective theory to describe the interlayer interaction for tBLG for small twist angles θ .

- [2] Lopes dos Santos JMB, Peres NMR and Neto AHC 2007 Graphene bilayer with a twist: electronic structure Phys. Rev. Lett. [99 256802](#)
- [3] Mele E J 2010 Commensuration and interlayer coherence in twisted bilayer graphene Phys. Rev. B [81 161405](#)
- [4] Trambly de Laissardière G, Mayou D and Magaud L 2010 Localization of Dirac electrons in rotated graphene bilayers Nano Lett. [10 804–8](#)
- [5] Shallcross S, Sharma S, Kandelaki E and Pankratov OA 2010 Electronic structure of turbostratic graphene Phys. Rev. B [81 165105](#)
- [6] Morell E S, Correa JD, Vargas P, Pacheco Mand Barticevic Z 2010 Flat bands in slightly twisted bilayer graphene: tight-binding calculations Phys. Rev. B [82 121407\(R\)](#)
- [7] Bistritzer R and MacDonald AH 2011 Moiré bands in twisted double-layer graphene Proc. Natl Acad. Sci. [108 12233](#)
- [8] Kindermann M and First PN 2011 Local sublattice-symmetry breaking in rotationally faulted multilayer graphene Phys. Rev. B [83 045425](#)
- [9] Xian L, Barraza-Lopez S and Chou MY 2011 Effects of electrostatic fields and charge doping on the linear bands in twisted graphene bilayers Phys. Rev. B [84 075425](#)
- [10] Lopes dos Santos JMB, Peres NMR and Neto AHC 2012 Continuum model of the twisted graphene bilayer Phys. Rev. B [86 155449](#)
- [11] Moon P and Koshino M 2013 Optical absorption in twisted bilayer graphene Phys. Rev. B [87 205404](#)
- [12] Moon P and Koshino M 2012 Energy spectrum and quantum hall effect in twisted bilayer graphene Phys. Rev. B [85 195458](#)
- [13] Moon P and Koshino M 2013 Optical properties of the hofstadter butterfly in the moiré superlattice Phys. Rev. B [88 241412](#)
- [14] Bistritzer R and MacDonald AH 2011 Moiré butterflies in twisted bilayer graphene Phys. Rev. B [84 035440](#)

Commensurate Superlattice & Moiré configurations over tBLG



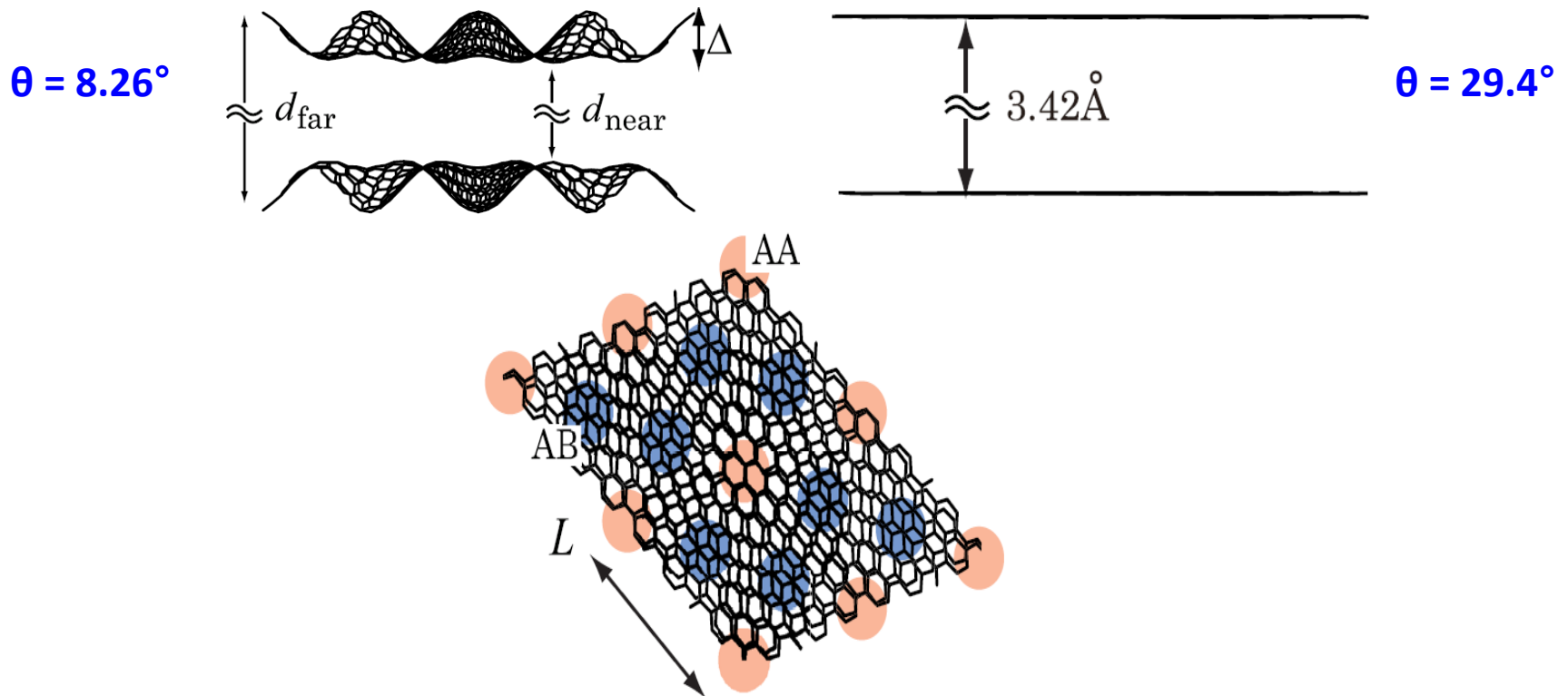
Moiré patterns do not necessarily exhibit a translational symmetry.

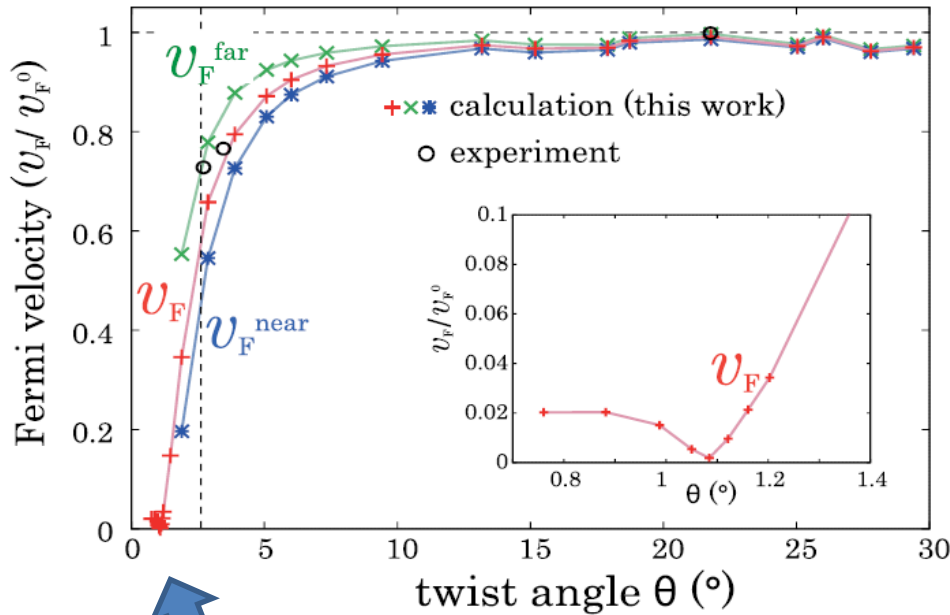
They are analyzed primarily for **small twist angles θ** ; when this is small and the Moiré length scale is much larger than the lattice constant, the interaction between the graphene layers in tBLG is dominated by long-wavelength (small-wavevectors) components, allowing to treat the problem in the effective continuum model.

Recent large-scale DFT calculations for tBLG

Oshiyama et al, J. App. Phys. 117 (2015) 112811

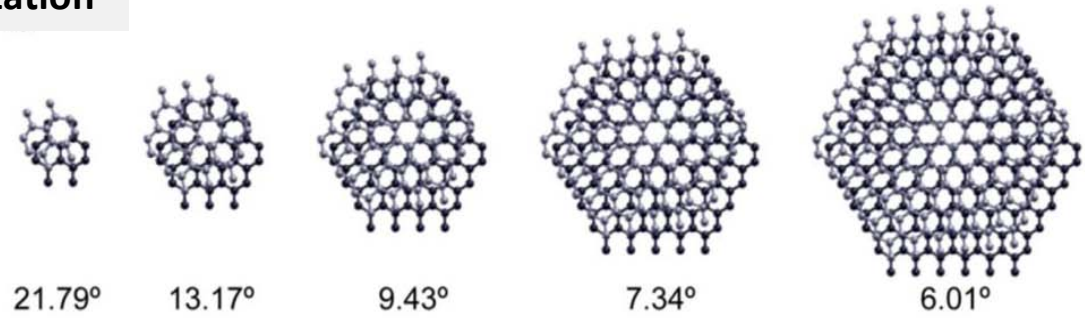
- Large-scale real-space finite-difference scheme allows to perform DFT calculations for nanometer-scale targets containing more than 100 000 atoms.
- The Moiré pattern induced by the mismatch over the tBLG drastically modifies the atomic and electronic structures.





Analyses of the Kohn-Sham orbitals clarify that the reason for the reduction of v_F and then the emergence of the flat bands is ascribed to the electron localization due to the Moiré pattern. For larger twist angle, the Kohn-Sham orbitals at E_F are characterized by π orbitals extending over the whole carbon sheet. However, when θ becomes as small as 1° , the Moiré pattern becomes prominent and the Kohn-Sham orbitals at E_F are localized in the AA stacking region. The Moiré pattern which becomes prominent for small θ induces inhomogeneity. The electron wave senses the inhomogeneity, and finally the Kohn-Sham orbitals are localized.

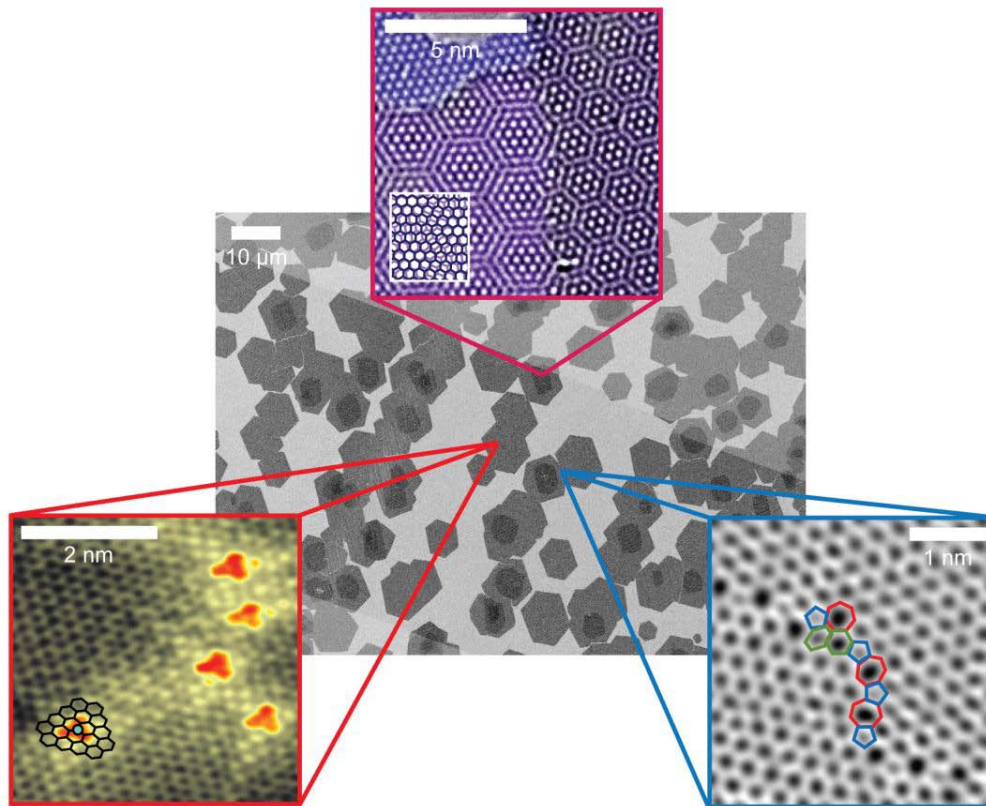
Moiré-induced electron localization



Moiré patterns

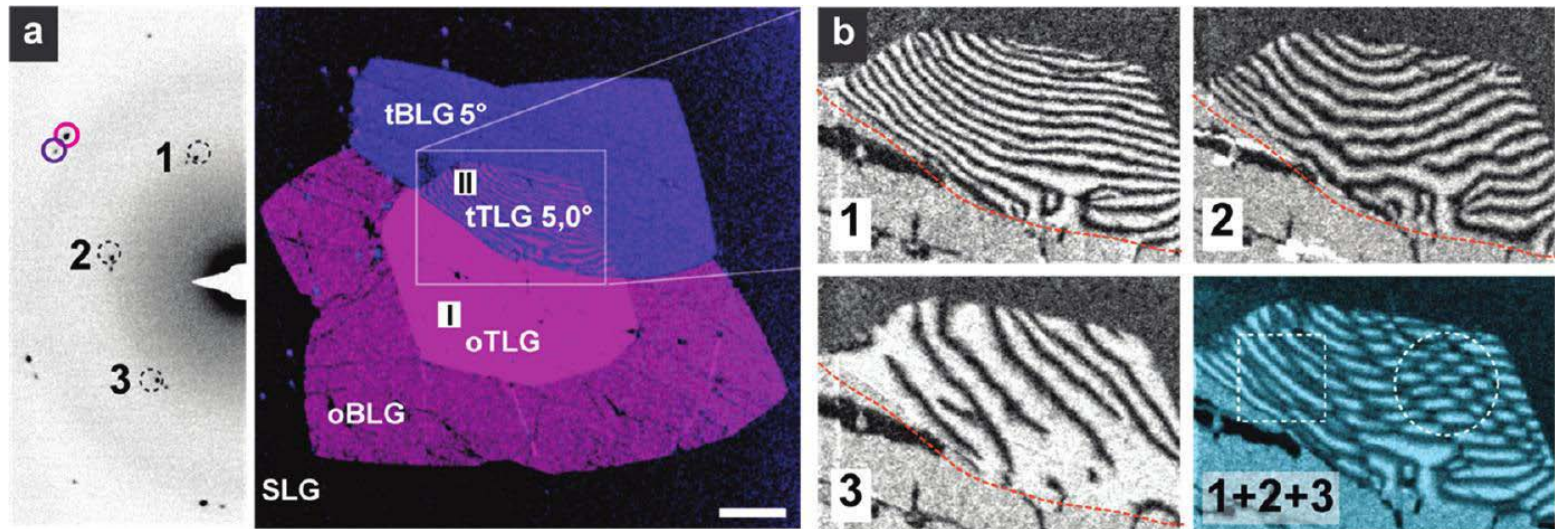
Intrinsic disorder in CVD graphene mono-layer

- Robin Havener, PhD thesis Cornell 2014, Imaging spectroscopy of heterogeneous two-dimensional materials
- Huang et al, doi:10.1038/nature09718



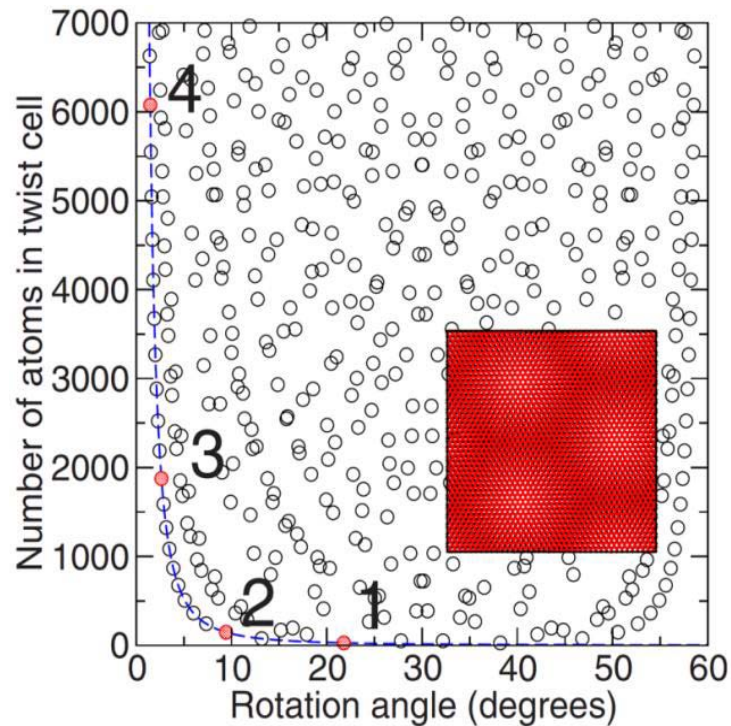
The scanning electron microscope (SEM) image in the **centre** illustrates the typical island growth of **CVD graphene on copper**; ultimately leading to:

- ▶ **grain boundaries (STEM image, right)** and
- ▶ **twisted multilayers (TEM image, top)** in the final material;
- ▶ **point defects (STM image, left)** can also be incorporated into the growth, either unintentionally or by design.



A DF-TEM image of **trilayer CVD graphene** in which the **top and bottom layers are very nearly oriented**, and the center layer is **slightly twisted**. The **complex Moiré patterns** between the top and bottom layers (b) show spatially varying strain, shear, **and rotation**.

Incommensurate configurations for tBLG

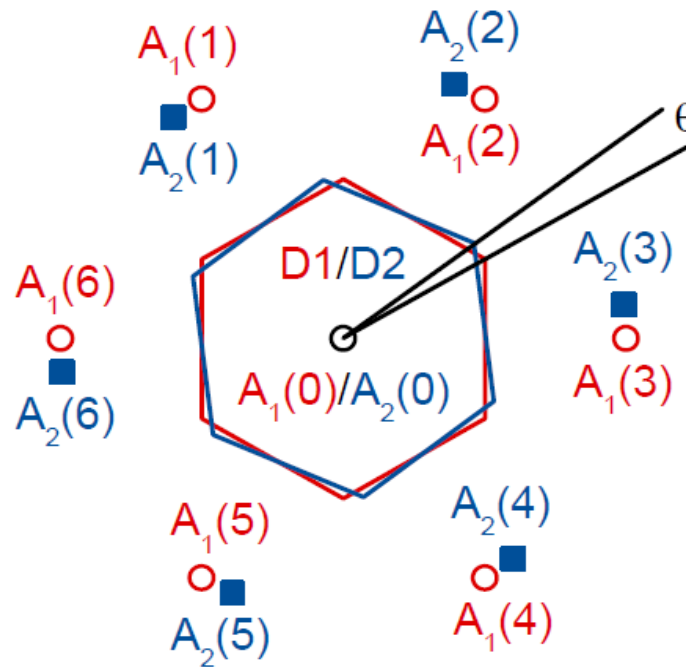


Shallcross et al, Phys. Rev. B 81
(2010) 165105

Size of unit cell versus θ in tBLG

Very small change in θ can lead to very large changes in unit cell size. The **minimum unit cell size (blue line) increases rapidly as θ decreases**, due to the large spatial period of the resulting Moiré pattern (inset).

Incommensurate tBLG for an arbitrary mismatch angle θ



The inequivalent points in domain D generate the quasi-infinite set of incommensurate configurations; D varies with mismatch angle θ .

Atom $A_1(0)$ is in layer 1. Atom $A_2(0)$ in layer 2 **can be at any position in its layer above $A_1(0)$ due to the interfacial incommensurate disorder**. Consequently D is **defined geometrically** as the set of inequivalent positions of $A_2(0)$.

If we place $A_2(0)$ at a point M outside this region, then by changing the choice of $A_1(0)$, we see that M is equivalent to a point inside region D . So considering a point outside D will not give a new configuration; it will only double count a given configuration.

Considering a single-orbital tight binding (TB) model for p_z atomic orbitals, the total electronic wavefunction

$$\begin{aligned}\Psi_{\mathbf{k}}(\mathbf{r}) &= C_{A_1}\Psi_{\mathbf{k};A_1}(\mathbf{r}) + C_{B_1}\Psi_{\mathbf{k};B_1}(\mathbf{r}) \\ &+ C_{A_2}\Psi_{\mathbf{k};A_2}(\mathbf{r}) + C_{B_2}\Psi_{\mathbf{k};B_2}(\mathbf{r})\end{aligned}$$

The restriction to the single p_z orbital per site yields $\rho\rho\pi$ in-plane and $\rho\rho\sigma$ interlayer bonds in the incommensurate tBLG system.

In the TB approach, solve the Schrödinger equation in matrix form to obtain the secular equation for the **λ electronic bands**

$$\det [H - E^\lambda(\mathbf{k})S] = 0$$

H and S denote respectively the Hamiltonian and overlap matrices

$$H = \begin{bmatrix} H_{11}(2 \times 2) & H_{12}(2 \times 2) \\ H_{21}(2 \times 2) & H_{22}(2 \times 2) \end{bmatrix} \quad \text{and} \quad H_{mn}(2 \times 2) = \begin{bmatrix} H_{A_m A_n} & H_{A_m B_n} \\ H_{B_m A_n} & H_{B_m B_n} \end{bmatrix}$$

Similarly for the S matrices.

1st stage: Real-space quasi-Hermitian virtual crystal VCA Hamiltonian for incommensurate tBLG systems

Through a numerical and statistical approach, analyze the incommensurate tBLG interface and its interlayer interactions for an arbitrary mismatch angle θ .

In particular, compute the **mean VCA for the interlayer interactions** between the referential sites $[\mathbf{A}_i(\mathbf{0}), \mathbf{B}_i(\mathbf{0})]$ in one layer interacting with the closest sites $[\mathbf{A}_j(n), \mathbf{B}_j(n)]$ in the other layer $i \neq j$, **in terms of average matrices**

$$\bar{H} = \begin{bmatrix} \bar{H}_{11} & \bar{H}_{A_1 A_2} Q \\ \bar{H}_{A_2 A_1} Q & \bar{H}_{22} \end{bmatrix} \quad \bar{H}_{A_1 A_2} = \sum_{n=0}^6 \bar{t}[A_1(0)A_2(n)] \times \exp [i(\overline{\mathbf{r}}_{A_2(n)} - \overline{\mathbf{r}}_{A_2(0)}) \cdot \mathbf{k}]$$

$$\bar{t}[A_1(0)A_2(n)] = \frac{\iint_{D_1} t(\|\mathbf{r}_{A_j(n)} - \mathbf{r}_{A_i(0)}\|) \Gamma(R_{\max} - \|\mathbf{r}_{A_j(n)} - \mathbf{r}_{A_i(0)}\|) dx dy}{\iint_{D_1} \Gamma(R_{\max} - \|\mathbf{r}_{A_j(n)} - \mathbf{r}_{A_i(0)}\|) dx dy}$$

\bar{t} (bar) average hopping interaction between closest sites on the layers 1 and 2.

2nd stage: Real-space Hermitian virtual crystal VCA Hamiltonian for incommensurate tBLG systems

The Hermiticity of the Hamiltonian operator describing the incommensurate tBLG in the TB-VCA approach may be retrieved by transposing the inner functional products in the Hamiltonian Hilbert space, for an arbitrary mismatch angle θ .

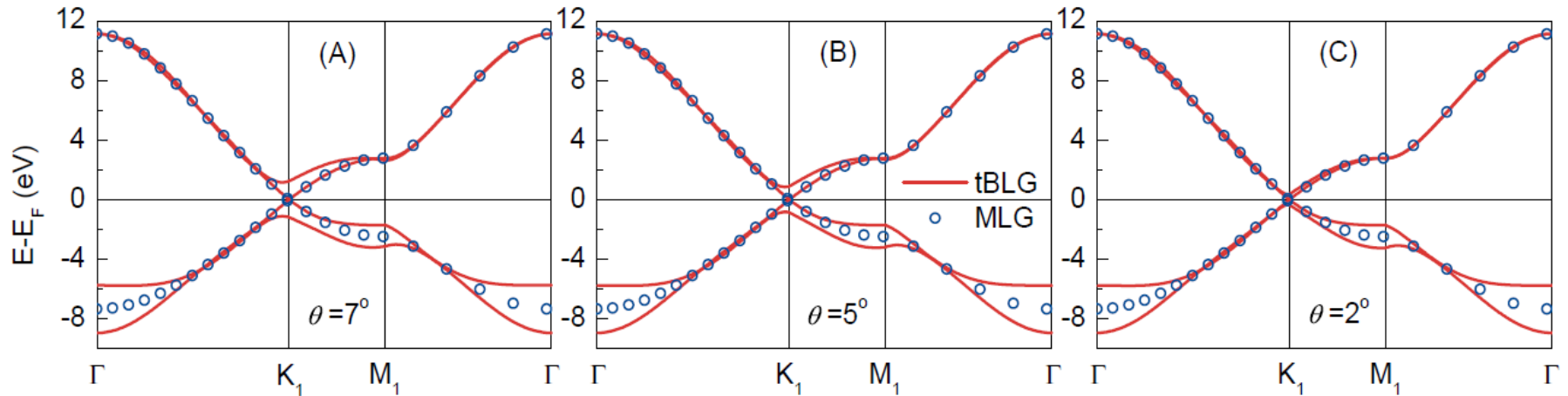
The **Hermitian Hamiltonian** \bar{H}' is computed as

$$\bar{H}' = \begin{bmatrix} (1 + \delta) \bar{H}_{11} & (\bar{H}_{A_1 A_2} + \bar{H}_{A_2 A_1}) Q \\ (\bar{H}_{A_1 A_2} + \bar{H}_{A_2 A_1}) Q & (1 + 1/\delta) \bar{H}_{22} \end{bmatrix}$$

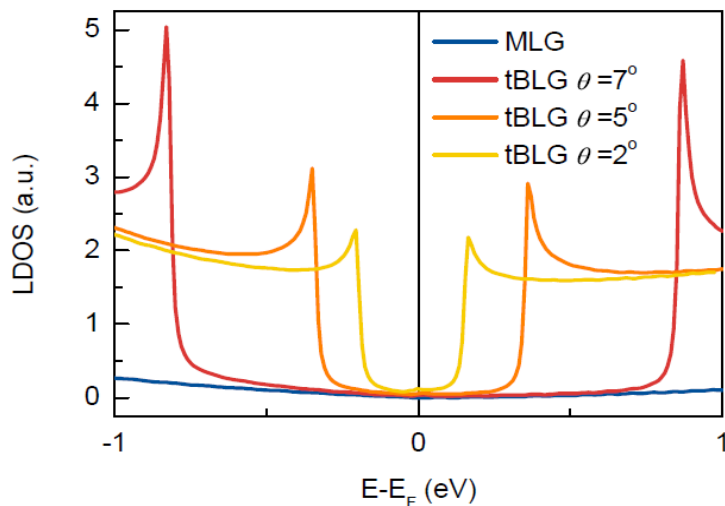
$$\delta = \bar{H}_{A_2 A_1} / \bar{H}_{A_1 A_2}$$

The quasi-Hermitian and Hermitian representations of the TB-VCA Hamiltonian operator are formally equivalent.

Calculated TB-VCA DOS for tBLG at lower energies for mismatch angles: $\theta = 7^\circ$, 5° , and 2°

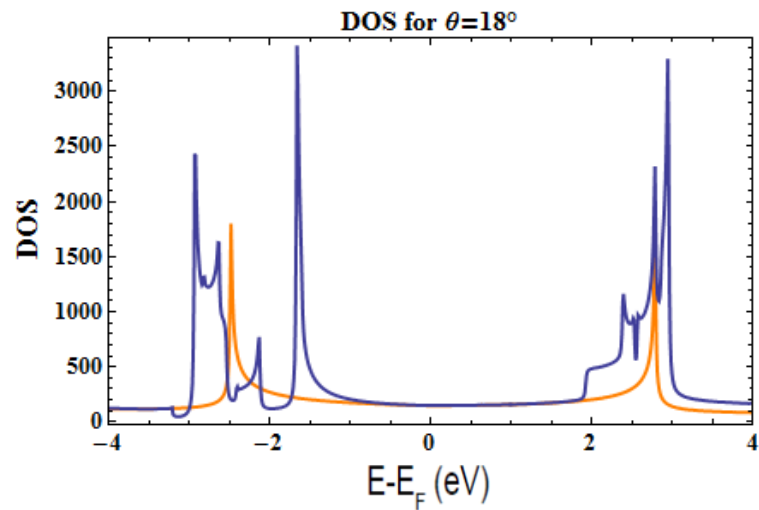
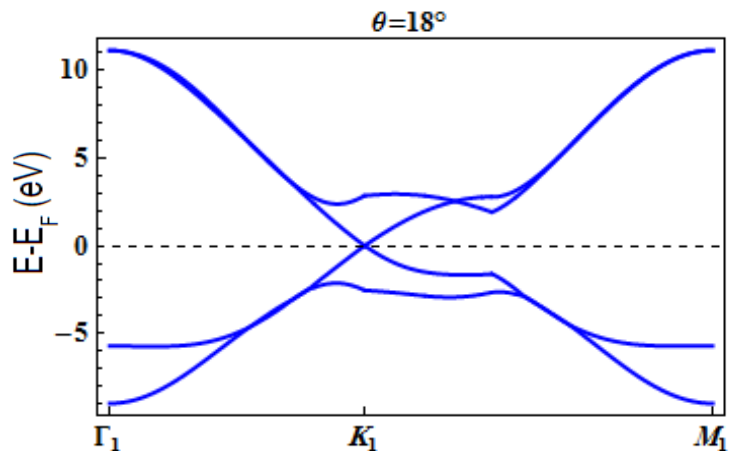
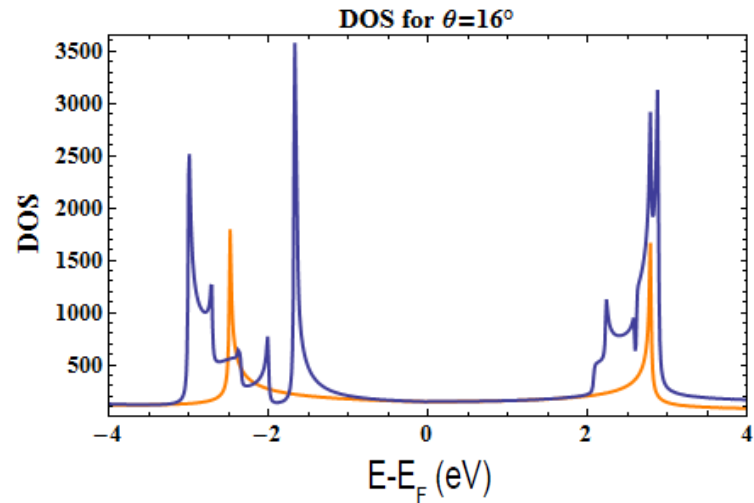
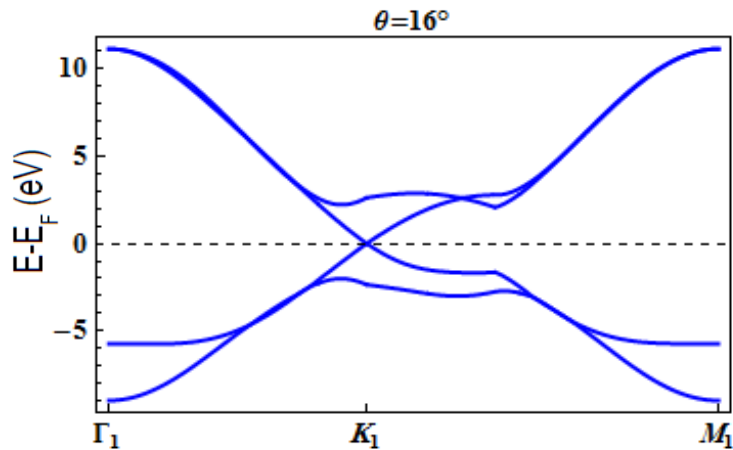


Calculated TB - VCA electronic band structures for tBLG with mismatch angles from left to right: $\theta = 7^\circ$, 5° , and 2° . Circles trace the electronic band structure of a single graphene layer.



Van Hove singularities (VHS) and corresponding **gaps** appear at **K** due to the tBLG structurally incommensurate layer bilayer interactions, which lift the local degeneracy. The **larger the mismatch** angle the **wider the gap**.

Calculated TB – VCA DOS for tBLG at extended energies for mismatch angles: $\theta = 16^\circ$ and 18° .



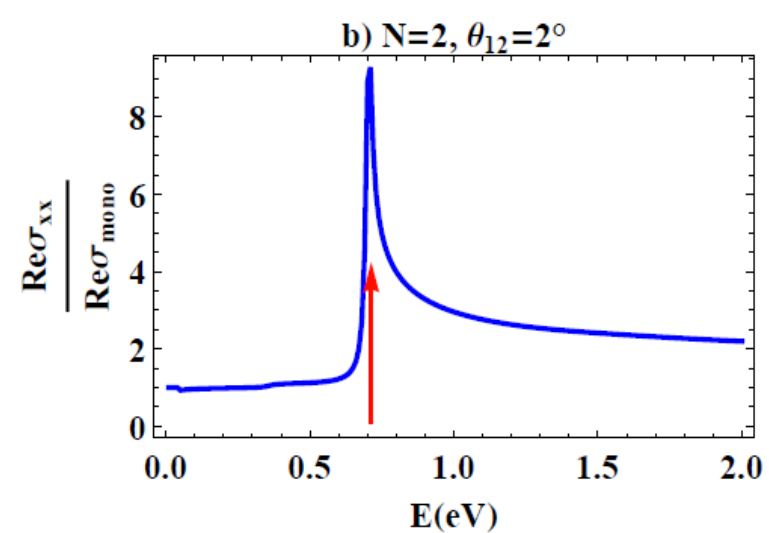
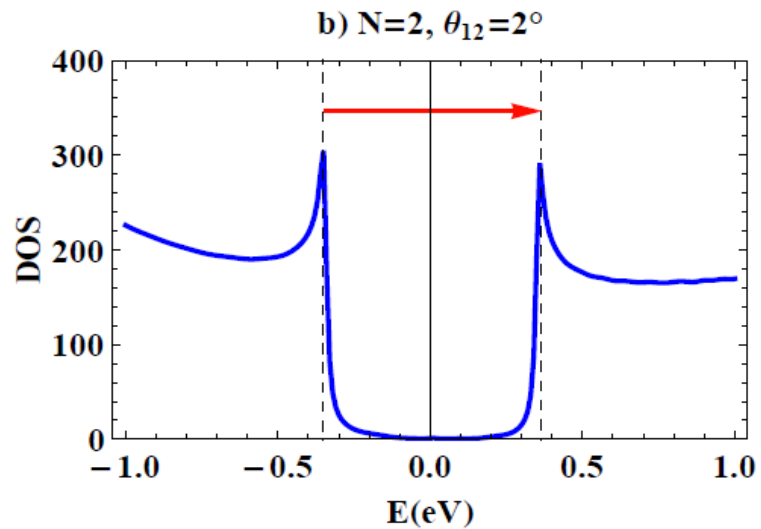
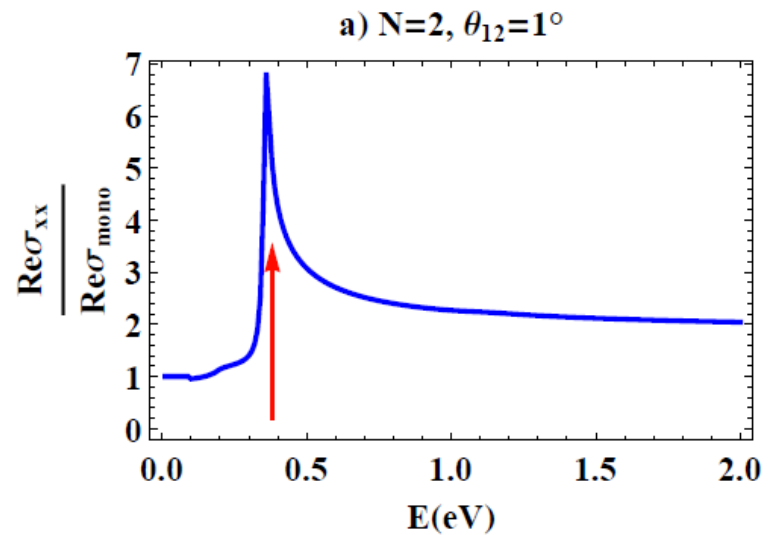
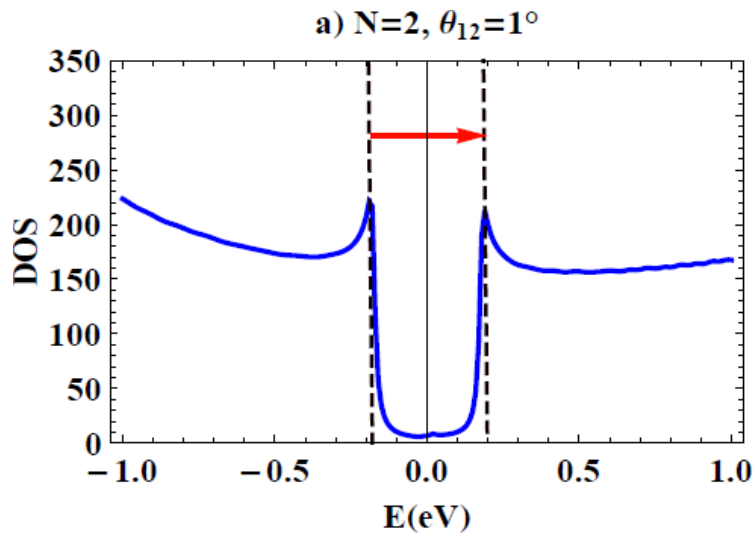
Calculated TB-VCA optical absorption spectra for incommensurate tBLG

The **optical absorption of light incident along the normal to the layers** of the **tBLG and tFLG systems**, is defined as the real part of the dynamic conductivity σ_{xx} , where the x-axis is in the plane of the layers. The dynamic conductivity may be calculated then along any given direction in the reciprocal space of the BZ for any of the graphene sheet layers in the system, using the Kubo formula

$$\sigma_{xx}(E) = i \frac{g_s g_v e^2}{\omega + i \epsilon} \int_{\Delta} \frac{dk}{2\pi} \sum_{\alpha, \beta} \frac{f(E_{\alpha}(\mathbf{k})) - f(E_{\beta}(\mathbf{k}))}{E - E_{\beta}(\mathbf{k}) + E_{\alpha}(\mathbf{k}) + i \epsilon} \times \langle \alpha, \mathbf{k} | \hat{j}_x | \beta, \mathbf{k} \rangle \langle \beta, \mathbf{k} | \hat{j}_x | \alpha, \mathbf{k} \rangle. \quad (2)$$

The constants \mathbf{g}_s and \mathbf{g}_v denote the spin and electronic valley degeneracies. \hat{j}_x is the **current operator** defined in the formalism as $\hat{j}_x = -\partial \hat{S}^{-1} \hat{H} / \partial k_x$ the real part of the **dynamic conductivity** σ_{xx} , where the x-axis is in the plane of the graphene layers. The $f(E_{\alpha}(\mathbf{k}))$ is the Fermi function, and $|\alpha, \mathbf{k}\rangle$ is the α sub-band eigenstate of the operator $\hat{S}^{-1} \hat{H}$ with **momentum** \mathbf{k} and **eigenstate** $E_{\alpha}(\mathbf{k})$.

Examples of TB-VCA calculated optical absorption spectra for incommensurate tBLG with mismatch angles: $\theta = 1^\circ$ and 2° .



1st order Umklapp processes in the reciprocal space of incommensurate tBLG

Mikito Koshino, New J. Phys. 17 (2015) 015014

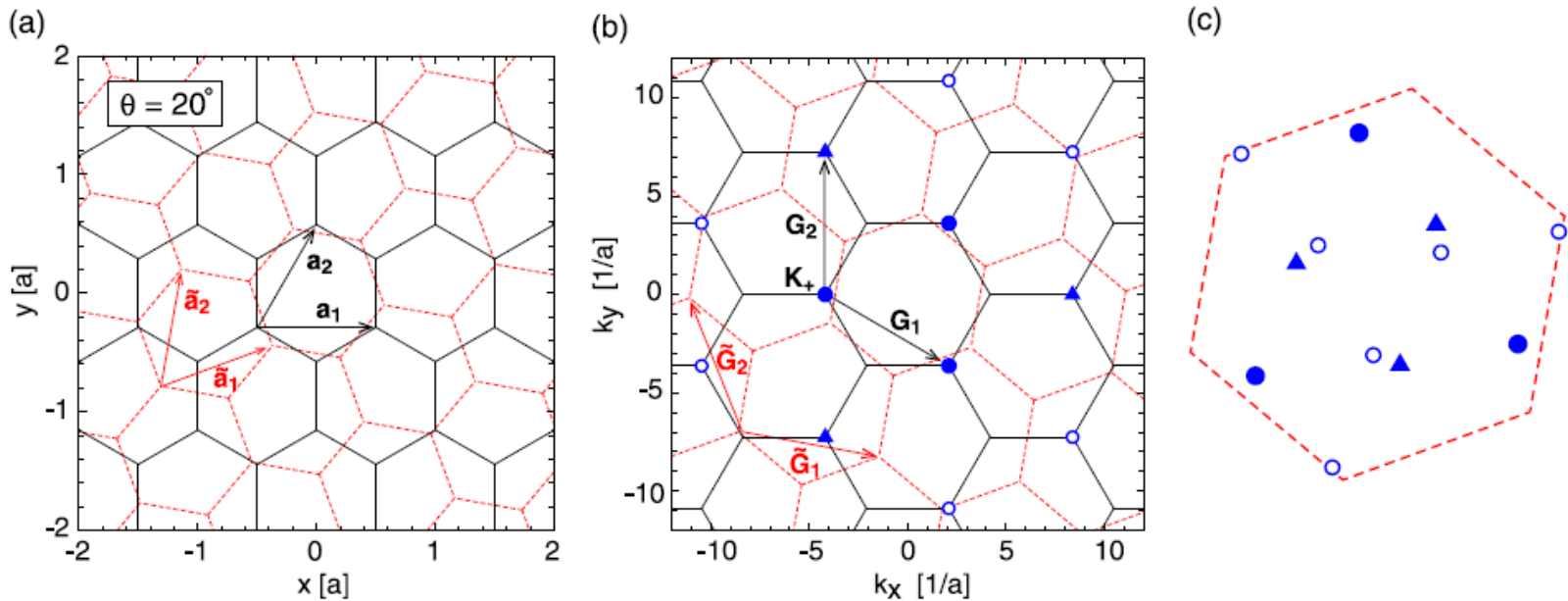
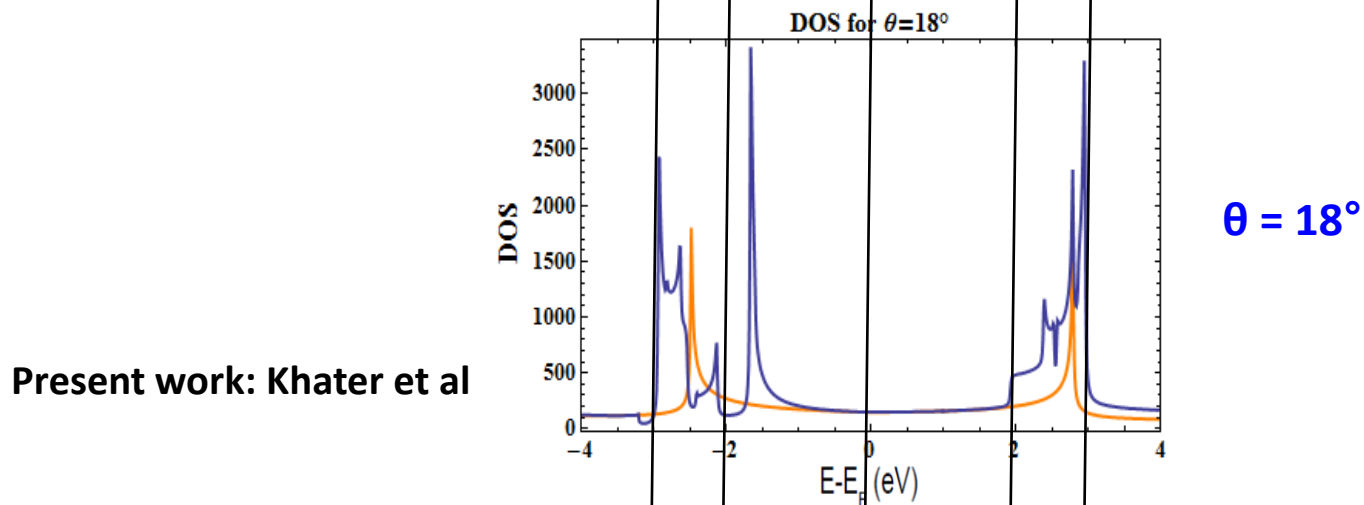
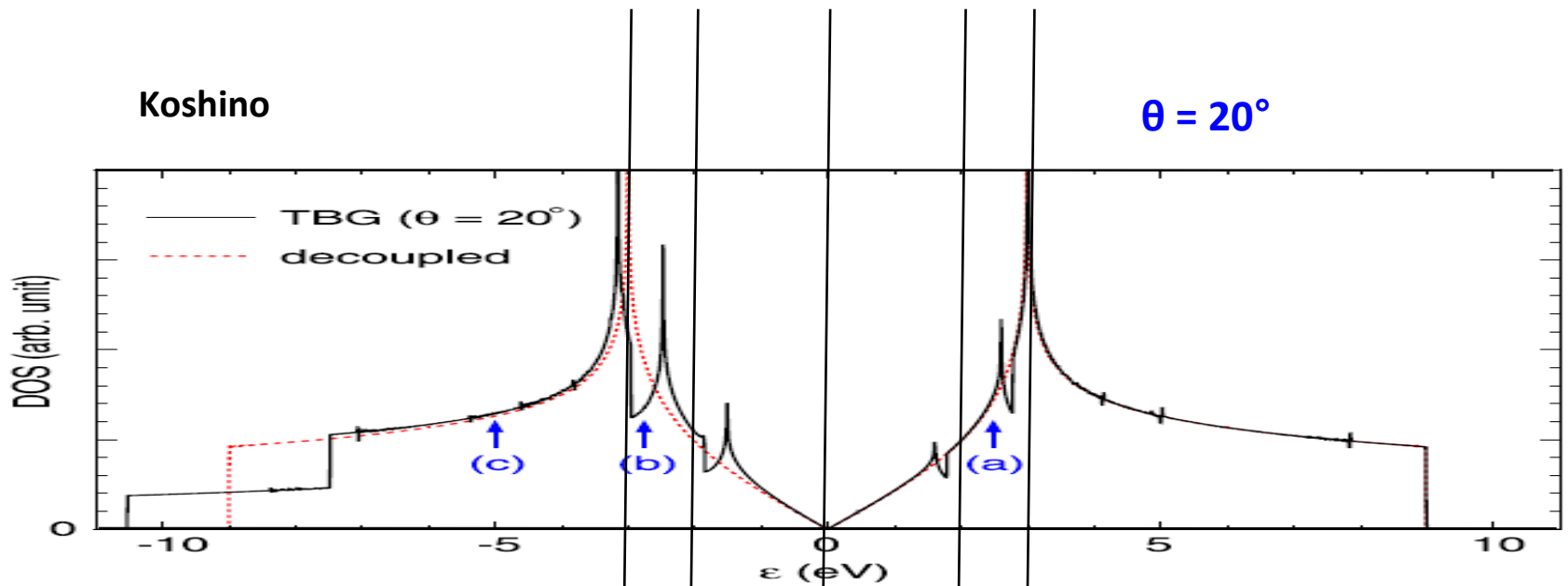


Figure 2. (a) Irregularly stacked bilayer graphene at rotation angle $\theta = 20^\circ$. (b) Brillouin zones of the individual layers in the extended zone scheme. Symbols (filled circles, triangles and open circles) represent the positions of $\mathbf{K}_+ + \mathbf{G}$ with several \mathbf{G} 's. The different symbols indicate the different distances from the origin. (c) Corresponding positions of the symbols in (b) inside the first Brillouin zone of layer 2.

The interlayer coupling is written in terms of the generalized Umklapp processes in the reciprocal space.

Koshino takes a vector in layer 1 to sample the vectors in the layer 2, to build up a DOS.

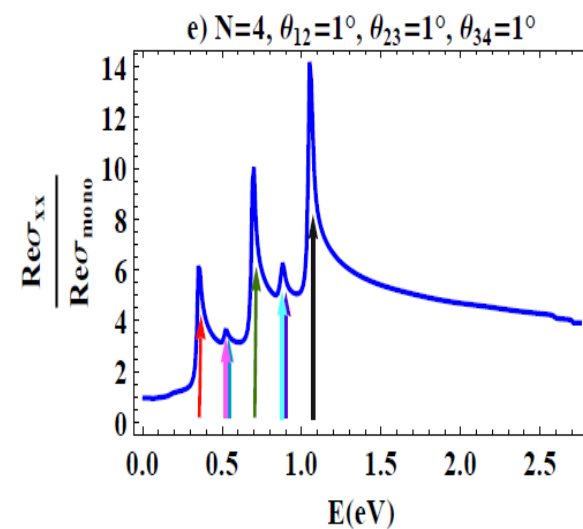
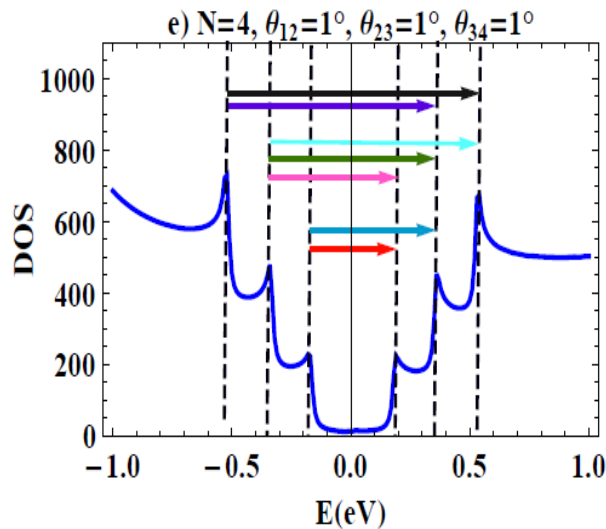
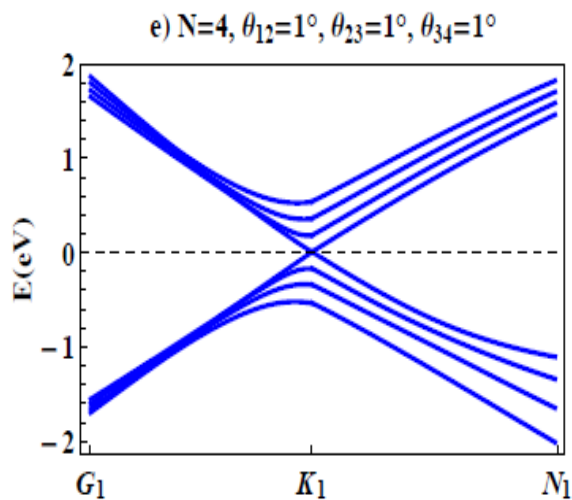
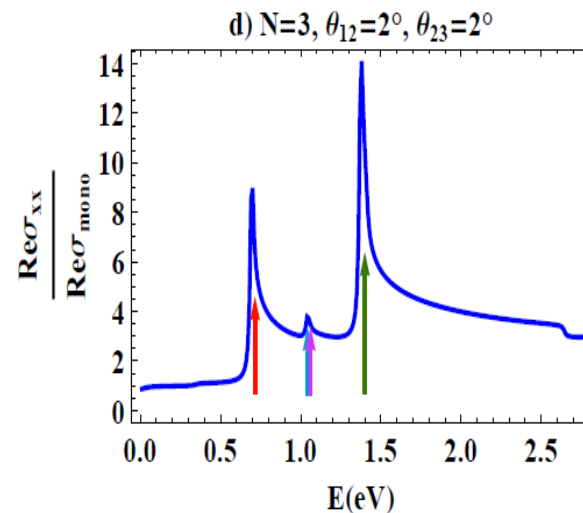
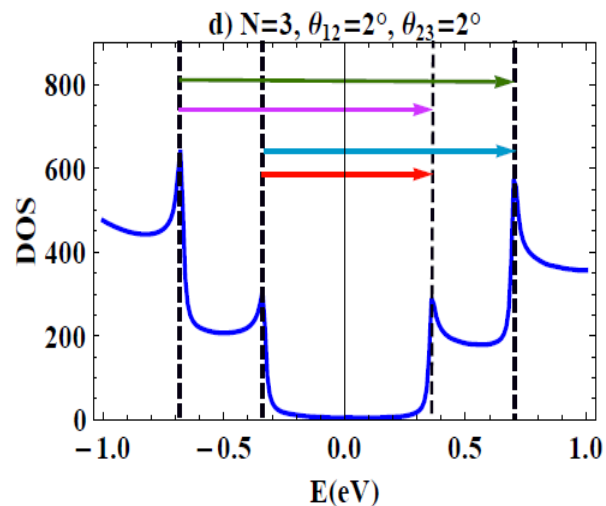
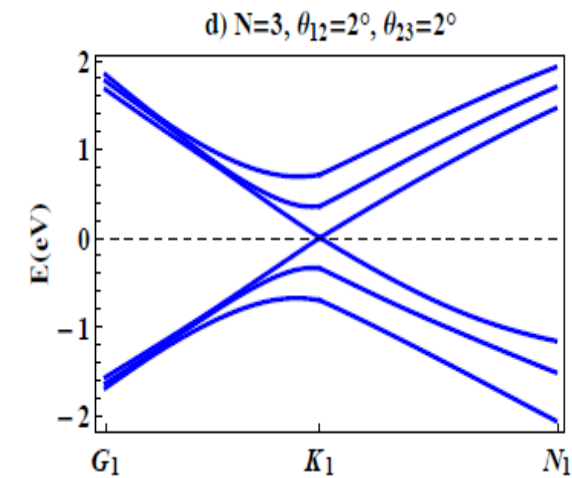


Comparison of both methods, they both use the single-orbital tight binding model for p_z atomic orbitals

tFLG systems

The TB – VCA method developed for the tBLG can be generalized directly to the tFLG systems

Examples for TB-VCA calculated electronic bands, DOS, and absorption spectra for tFLG systems, at small mismatch angles



Conclusions

- We have developed a general TB-VCA method to investigate and compute the electronic dynamics, and the light absorption spectra, for incommensurate graphene tBLG and tFLG nanostructured systems.
- If technically optimized, the tFLG heterostructures with a limited number of graphene mono layers (say $n < 6$) at random interlayer twist angles, present potential applications for tandem solar cells.
- The method can be developed to study the ballistic electronic transport across the incommensurate interfaces of such systems using the DNLCPA.



Computational Materials Physics group 2015, IMMM UMR6283, Université du Maine, France, left to right: M. Chebil, D. Ghader, A. Parii, L. Abou Khaleel, O. Nafa, A. Khater, R. Tigrine, D. Szczyński, V. Ashokan, B. Bourahla.